Passive Realtime Datacenter Fault Detection and Localization

Arjun Roy, ***University of California, San Diego;***
Hongyi Zeng and Jasmeet Bagga, ***Facebook;***
Alex C. Snoeren, ***University of California, San Diego***

https://www.usenix.org/conference/nsdi17/technical-sessions/presentation/roy

This paper is included in the Proceedings of the 14th USENIX Symposium on Networked Systems Design and Implementation (NSDI '17).

March 27–29, 2017 • Boston, MA, USA

ISBN 978-1-931971-37-9

Open access to the Proceedings of the 14th USENIX Symposium on Networked Systems Design and Implementation is sponsored by USENIX.

Passive Realtime Datacenter Fault Detection and Localization

Arjun Roy, Hongyi Zeng†, Jasmeet Bagga†, and Alex C. Snoeren

UC San Diego and †Facebook, Inc.

ABSTRACT

Datacenters are characterized by their large scale, stringent reliability requirements, and significant application diversity. However, the realities of employing hardware with small but non-zero failure rates mean that datacenters are subject to significant numbers of failures, impacting the performance of the services that rely on them. To make matters worse, these failures are not always obvious; network switches and links can fail partially, dropping or delaying various subsets of packets without necessarily delivering a clear signal that they are faulty. Thus, traditional fault detection techniques involving end-host or router-based statistics can fall short in their ability to identify these errors.

We describe how to expedite the process of detecting and localizing partial datacenter faults using an end-host method generalizable to most datacenter applications. In particular, we correlate transport-layer flow metrics and network-I/O system call delay at end hosts with the path that traffic takes through the datacenter and apply statistical analysis techniques to identify outliers and localize the faulty link and/or switch(es). We evaluate our approach in a production Facebook front-end datacenter.

1. INTRODUCTION

Modern datacenters continue to increase in scale, speed, and complexity. As these massive computing infrastructures expand—to hundreds of thousands of multi-core servers with 10- and 40-Gbps NICs [35] and beyond—so too do the sets of applications they support: Google recently disclosed that their datacenter network fabrics support literally thousands of distinct applications and services [37]. Yet the practicality of operating such multi-purpose datacenters depends on effective management. While any given service might employ an army of support engineers to ensure its efficient operation, these efforts can be frustrated by the inevitable failures that arise within the network fabric itself.

Unfortunately, experience indicates that modern datacenters are rife with hardware and software failures—indeed, they are designed to be robust to large numbers of such faults. The large scale of deployment both ensures a non-trivial fault incidence rate and complicates the localization of these faults. Recently, authors from Microsoft described [44] a rogue's gallery of datacenter faults: dusty fiber-optic connectors leading to corrupted packets, switch software bugs, hardware faults, incorrect ECMP load balancing, untrustworthy counters, and more. Confounding the issue is the fact that failures can be intermittent and partial: rather than failing completely, a link or switch might only affect a subset of traffic, complicating detection and diagnosis. Moreover, these failures can have significant impact on application performance. For example, the authors of NetPilot [42] describe how a single link dropping a small percentage of packets, combined with cut-through routing, resulted in degraded application performance and a multiple-hour network goose chase to identify the faulty device.

Existing production methods for detecting and localizing datacenter network faults typically involve watching for anomalous network events (for example, scanning switch queue drop and link utility/error counters) and/or monitoring performance metrics at end hosts. Such methods consider each event independently: "Did a drop happen at this link? Is application RPC latency unusually high at this host?" Yet, in isolation, knowledge of these events is of limited utility. There are many reasons an end host could observe poor network performance; similarly, in-network packet drops may be the result of transient congestion rather than a persistent network fault. Hence, datacenter operators frequently fall back to active probing and a certain degree of manual analysis to diagnose and localize detected performance anomalies [19, 44].

Instead, we propose an alternative approach: rather than looking at anomalies independently, we consider the impacts of faults on aggregate application performance. Modern datacenter fabrics are designed with a plethora of disjoint paths and operators work hard to load balance traffic across both paths and servers [9, 37]. Such designs result in highly regular flow performance regardless of path—in the absence of network faults [35]. An (unmitigated) fault, on the other hand, will manifest itself as a performance anomaly visible to end hosts. Hence, to detect faults, we can compare performance end hosts observe along different paths and hypothesize that outliers correspond to faults within the network.

To facilitate such a comparison, we develop a lightweight packet-marking technique—leveraging only forwarding rules supported by commodity switching ASICs—that uniquely identifies the full path that a packet traverses in a Facebook datacenter. Moreover,

the topological regularity of Facebook's datacenter networks allows us to use path information to passively localize the fault as well. Because each end host can bin flows according to the individual network elements they traverse, we can contrast flows traversing any given link (switch) at a particular level in the hierarchy with flows that traverse alternatives in order to identify the likely source of detected performance anomalies. Operators can then use the output of our system—namely the set of impacted traffic and the network element(s) seemingly responsible—in order to adjust path selection (e.g., through OpenFlow rules, ECMP weight adjustment [32], or tweaking inputs to flow hashes [23]) to mitigate the performance impact of the fault until they can repair it.

A naive implementation of our approach is unlikely to succeed given the noisiness of flow-based metrics at individual host scale. Furthermore, distinct applications, or different workloads for the same application, are likely to be impacted differently by any given fault. Here the massive scale of modern datacenters aids us: Specifically, when aggregated across the full set of traffic traversing any given network link, we find that statistical techniques are effective at using end-host-based metrics to identify under-performing links in real time. Our experience suggests this can remain true even when end hosts service different requests, communicate with disjoint sets of remote servers, or run entirely distinct application services.

To be practical, our approach must not place a heavy burden on the computational resources of either end hosts or the network switches, and neither can we require significant network bandwidth or esoteric features from the switches themselves. Furthermore, our analysis techniques must avoid false positives despite the diversity and scale of production datacenters yet remain sensitive to the myriad possible impacts of real-word faults. Our contributions include (1) a general-purpose, end-host-based performance monitoring scheme that can robustly identify flows traversing faulty network components, (2) a methodology to discover the necessary path information scalably in Facebook's datacenters, and (3) a system that leverages both types of information in aggregate to perform network-wide fault-localization.

At a high level, while network statistics can be noisy and confusing to interpret in isolation, the regular topology and highly engineered traffic present within Facebook's datacenters provides an opportunity to leverage simple statistical methods to rapidly determine where partial faults occur as they happen. We demonstrate that our technique is able to identify links and routers exhibiting low levels (0.25–1.0%) of packet loss within a Facebook datacenter hosting user-servicing front-end web and caching servers within 20 seconds of fault occurrence with a minimal amount of processing overhead. We also perform a sensitivity analysis on a testbed to consider different types of errors—including those that induce only additional latency and not loss—traffic patterns, application mixes, and other confounding factors.

2. MOTIVATION & RELATED WORK

While fault detection is a classical problem in distributed systems [7, 11, 13, 14, 18, 33] and networks [12, 24, 29], modern datacenter environments provide both significant challenges (e.g., volume and diversity of application traffic, path diversity, and stringent latency requirements) and benefits (large degree of control, regular topologies) that impact the task of effectively finding and responding to network faults. Moreover, recent work has indicated that the types and impacts of faults common in modern datacenters [42, 44] differ from those typically encountered in the wide-area [34, 40] and enterprise [39].

Datacenters are affected by a menagerie of errors, including a mix of software errors (ECMP imbalances, protocol bugs, etc.), hardware errors (packet corruption due to cables or switches, unreliable packet counters, bit errors within routing tables, etc.), configuration errors, and a significant number of errors without an apparent cause [44]. Errors can be classed into two main categories: a complete error, in which an entire link or switch is unable to forward packets, or a partial error, where only a subset of traffic is affected. In this work, we focus primarily on the latter. Even a partial error affecting and corrupting only 1% of packets on two links inside a datacenter network was noted to have a $4.5\times$ increase in the 99th-percentile application latency [42], which can impact revenue generated by the hosted services [21].

Commonly deployed network monitoring approaches include end-host monitoring (RPC latency, TCP retransmits, etc.) and switch-based monitoring (drop counters, queue occupancies, etc.). However, such methods can fall short for troubleshooting datacenter scale networks. Host monitoring alone lacks specificity in the presence of large scale multipath; an application suffering from dropped packets or increased latency does not give any intuition on where the fault is located, or whether a given set of performance anomalies are due to the same fault.

Similarly, if a switch drops a packet, the operator is unlikely to know which application's traffic was impacted, or, more importantly, what is to blame. Even if a switch samples dropped packets the operator might not have a clear idea of what traffic was impacted. Due to sampling bias, mouse flows experiencing loss might be missed, despite incurring great impacts to performance. (We expound upon this issue in Appendix A.) Switch-counter-based approaches are further confounded by cut-through forwarding and unreliable hardware [44].

Thus, we propose a system that focuses not on the occurrence of network anomalies but rather on their impact on traffic. In doing so we leverage the high path diver-

sity and regular topologies found in modern datacenters, as well as the finely tuned load balancing common in such environments. We also expose to each host, for every flow, the path taken through the network. As such, our approach has several key differences with both past academic proposals and production systems:

1. **Full path information**: Past fault-finding systems have associated performance degradations with components and logical paths [7, 10, 13, 19] but a solution that correlates performance anomalies with specific network elements for arbitrary applications has, to the best of our knowledge, proved elusive—although solutions exist for carefully chosen subsets of traffic [44].
2. **Passive monitoring, not active probing**: In contrast to active probing methods [17, 19], our method leverages readily available metrics from production traffic, simultaneously decreasing network overhead, increasing the detection surface, and decreasing detection and localization time.
3. **Reduced switch dependencies**: While some approaches require expanded switch ASIC features for debugging networks [20], we do not require them. This allows network operators to deploy our approach on commodity switches, and makes our approach resilient to bugs that may escape on-switch monitoring.
4. **No per-application modeling:** Our system leverages the stable and load-balanced traffic patterns found in some modern datacenters [35]. Thus, it does not need to model complicated application dependencies [7, 11, 13] or interpose on application middleware [14]. Since we compare relative performance across network links, we do not require explicit performance thresholds.
5. **Rapid online analysis**: The regularity inherent in several academic [8] and production [9, 37] topologies allow us to simplify our analysis to the point that we can rapidly (10–20 seconds) detect partial faults of very small magnitude ($\leq$ 0.5% packet loss) using an online approach. This contrasts with prior systems that require offline analysis [7] or much larger timescales to find faults [11]. Furthermore, localizing faults is possible without resource-intensive and potentially time consuming graph analysis [17, 24, 25, 26, 27, 30].

3. SYSTEM OVERVIEW

In this section, we present the high-level design of a system that implements our proposed approach. To set the context for our design, we first outline several important characteristics of Facebook's datacenter environment. We then introduce and describe the high-level responsibilities of the three key components of our system, deferring implementation details to Section 4.

3.1 Production datacenter

Facebook's datacenters consist of thousands of hosts and hundreds of switches grouped into a multi-rooted, multi-level tree topology [9]. The datacenter we consider serves web requests from a multitude of end users, and is comprised primarily of web servers and cache servers [35]. While wide-area connections to other installations exist, we do not focus on those in this work.

3.1.1 Topology

Web and cache hosts are grouped by type into racks, each housing a few tens of hosts. User requests are load balanced across all web servers, while cached objects are spread across all caches. Since any web server can service any user request, there is a large fan-out of connections between web servers and caches; in particular, each web server has thousands of bidirectional flows spread evenly amongst caches [35]. Prior work notes both the prevalence of partition-aggregate workloads and the detrimental impact of packet loss and delay in this latency sensitive environment—even if they only constitute the long tail of the performance curve [43].

A few tens of racks comprises a pod. Each pod also contains four aggregation switches (Aggs). Each ToR has four uplinks, one to each Agg. There are a few tens of pods within the datacenter, with cross-pod communication enabled by four disjoint planes of core switches (each consisting of a few tens of cores). Each Agg is connected to the cores in exactly one plane in a mesh.

Each host transmits many flows with differing network paths. Due to the effects of ECMP routing, mesh-like traffic patterns, and extensive load balancing, links at the same hierarchical level of the topology end up with a very even distribution of a large number of flows. Moreover, if we know which path (i.e., set of links) every flow traverses, it is straightforward to separate the flows into bins based on the link they traverse at any particular level of the hierarchy. Hence, we can simultaneously perform fault identification and localization by considering performance metrics across different subsets of flows.

3.1.2 Operational constraints

The sheer scale of the datacenter environment imposes some significant challenges on our system. The large number of links and switches require our system to be robust to the presence of multiple simultaneous errors, both unrelated (separate components) and correlated (faults impacting multiple links). While some errors might be of larger magnitude than others, we must still be sensitive to the existence and location of the smaller errors. In addition, we must detect both packet loss and delay.

The variety of applications and workloads within the datacenter further complicate matters—an improper choice of metric can risk either masking faults or triggering false positives (for example, the reasonable sounding choice of request latency is impacted not only by net-

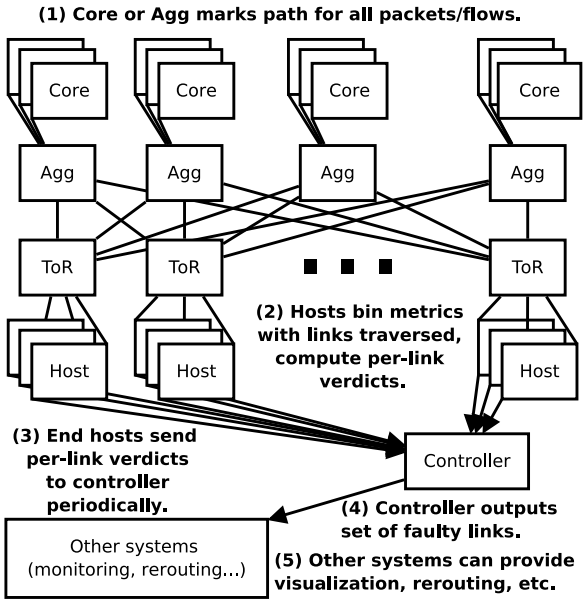

Figure 1: High-level system overview (single pod depicted).

work faults but also cache misses, request size and server loads). Moreover, datacenters supporting multiple tenants clearly require application-agnostic metrics.

Furthermore, we must be able to support measurements from large numbers of end hosts describing the health of a large number of links, without imposing large computational or data overheads either on the end hosts or on the network. This is especially true of network switches, where relatively under-provisioned control planes are already engaged in critical tasks including BGP routing. Thus, we are limited to capabilities present in the data planes of commodity switch ASICs.

3.2 System architecture

Our fault detection and localization approach involves functional components at all end hosts, a subset of switches, and a centralized controller, depicted in Figure 1. Switches mark packets to indicate network path (1). Hosts then independently compare the performance of their own flows to generate a host-local decision about the health of all network components (2). These *verdicts* are sent (3) to a central controller, which filters false positives to arrive at a final set of faulty components (4), which may be further acted upon by other systems (5). We expand on the role of each element below.

3.2.1 End hosts

Hosts run production application traffic and track various per-flow metrics detailed in Section 4.2. In addition, the host is aware of each flow's path through the network. Periodically, hosts will use collected performance data to issue verdicts for whether it considers a given subset of flows to have degraded performance, or not. By default, flow metrics are binned by the set of links they traverse. These bins are then further grouped into what we call *equivalence sets* (ESes), i.e., the set of bins that should perform equivalently, allowing us to pinpoint link-level faults. In the Facebook datacenter, the set of bins corresponding to the downlinks from the network core into a pod forms one such ES. Alternative schemes can give us further resolution into the details of a fault: for example, comparing traffic by queue or subnet (Section 5.4.4). We discuss the impact of heterogeneous traffic and topologies on our ability to form ESes in Section 6.

We define a *guilty* verdict as an indication that a particular bin has degraded performance compared to others in its ES; a *not guilty* verdict signifies typical performance. We leverage path diversity and the ability to compare performance across links—if every link in an ES is performing similarly, then either none of the links are faulty, all of them are faulty (unlikely in a production network) or a fault exists but might be masked by some other bottleneck (for which we cannot account). The target case, though, is that enough links in an ES will be fault-free at any given moment, such that the subset of links experiencing a fault will be readily visible if we can correlate network performance with link traversed. Even in the absence of path diversity (e.g., the access link for a host) we can use our method with alternative binning schemes and equivalence sets to diagnose certain granular errors.

3.2.2 Switches

A subset of the network switches are responsible for signaling to the end hosts the network path for each flow; we describe details in Section 4.1. Once faults are discovered by the centralized controller, switches could route flows away from faulty components, relying on the excess capacity typically found in datacenter networks. We leave fault mitigation to future work.

3.2.3 Controller

In practice, there will be some number of false positives within host-generated verdicts for link health (e.g. hosts flagging a link that performs poorly even in the absence of an error, possibly due to momentary congestion) confounding the ability to accurately deliver fixes to the network. Furthermore, there might be errors which do not affect all traffic equally; for example, only traffic from a certain subnet might be impacted, or traffic of a certain class. Hence, we employ a central controller that aggregates end-host verdicts for links (or other bins) into a single determination of which links—if any—are suffering a fault. In addition, the controller can drive other administrative systems, such as those used for data visualization/logging or rerouting of traffic around faults. Such systems are outside the scope of this work.

4. IMPLEMENTATION

We now present a proof-of-concept implementation that meets the constraints presented above. In order, we focus on scalable path signalling, our choice of end-host

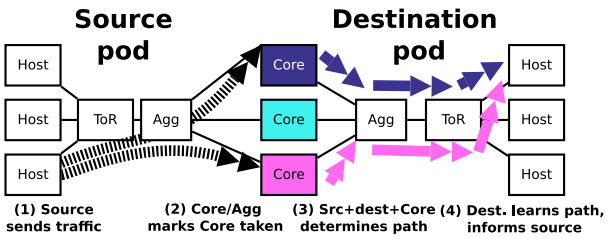

Figure 2: Determining flow network path.

performance metrics and the required aggregation processing, our verdict generator for aggregated flow metrics, and the operation of our centralized controller.

4.1 Datacenter flow path discovery

Central to our approach is the ability to scalably and feasibly discover flow path information within the datacenter. While switch CPU/dataplane limits complicate this task, the regularity of the network topology aids us.

4.1.1 Topological constraints

Figure 2 depicts the pathfinding scheme we use in the Facebook datacenter. To aid discussion, the diagram shows a restricted subset of an unfolded version of the topology, with source hosts on the left and destinations on the right; the topology is symmetric so our approach works in either direction. Note that cross-pod traffic has only two ECMP decisions to make: which Agg switch (and thus, core plane) to transit after the ToR, and which core switch to use within the core plane. Each core plane is only connected to one Agg switch per pod, so the destination Agg switch is fixed given the core plane.

The source and destination racks and ToRs are fixed for any particular host pair, and can be determined by examining the IP addresses of a flow. Thus, for cross-pod traffic, the choice of core switch uniquely determines the flow's path, as the Agg switches are then constrained on both sides. For intra-pod traffic it suffices to identify the Agg switch used to connect the ToRs.

In the presence of a total link error, the network attempts to forward traffic using an alternative, non-shortest path advertised as a backup route. While we do not address this case in our proof of concept, we discuss the impacts of link failures in Section 6.3.

4.1.2 Packet marking

We assign an ID to each core switch, that is stamped on all packets traversing the switch. Note that the stamp need not be inserted by the core switch itself—the Agg switches on either side are also aware of the core's identity and are equally capable of marking the packet. We use Linux eBPF (Extended Berkeley Packet Filter) [3] along with `bcc` (BPF Compiler Collection) [2] instrumentation at end hosts to read packet markings and derive flow paths. Our naive implementation imposes less than 1% CPU overhead (top row of Table 2), but room for optimization remains.

Several candidate header fields can be used for marking, and the best choice likely depends on the details of any given deployment. One possibility is the IPv6 flow label field; a 20-bit ID could scale to a network with over a million core switches. However, the ASIC in our Agg switches does not currently support modifying this field. Thus, for our proof of concept, we instead mark the IPv6 DSCP field, which is supported at line rate and requires only a constant number of rules (one per uplink).

While DSCP suffices for a proof of concept, its length limits the number of discernible paths. Furthermore, datacenter operators often use DSCP to influence queuing, limiting the available bits. One alternative is to mark the TTL field[1]. A packet marked at a downward-facing Agg traverses exactly two more hops before arriving at the destination host; a host could recover an ID in the TTL field as long as the value was in the range 3–255.

4.1.3 General case

More complex topologies might preclude our ability to compute paths from a single stamp. In the event that traffic is made up of long-lived flows (as it is, for example, for the web and cache servers we tested) we can leverage the match/mark capability that many switching ASICs possess to implement a form of marking reminiscent of previous proposals for IP traceback [36].

Suppose there are H hops between source and destination system, and C routing choices per hop. If we want to determine the path taken by a flow at the first hop where a routing choice must be made, the operating system can mark C packets, each with the IPv6 flow label set to the possible IDs of each switch that the packets could transit for that hop. Switches would be configured with a single rule that would examine the flow label—if it matches the switch ID, the switch would set a single DSCP bit to 1. When the end host receiving the packet notes the DSCP bit set to 1, it could signal the sender with the ID of the switch that was transited at that hop (that is, the flow label of the packet when the DSCP bit was set). For example, it could do this by setting a specific DSCP bit in the ACK packet while setting the flow label of the return packet to the switches ID. Thus, if the flow sends $\geq (H \cdot C)$ packets in total it can discover the entire path, at the expense of just a single rule per switch. While we have not deployed this approach in production, we validated that our switch hardware can implement it. While this method finds out path information hop by hop, partial path information can still be useful to our system. We discuss this further in Section 6.4.

4.2 Aggregating host metrics & path data

Given the availability of per-flow path information, we show that both transport-layer and system-call-timing

[1]Constraints exist on the use of TTL as well, such as in the presence of `traceroute` or eBGP session protection [15].

metrics can be used to find under-performing links in real-world scenarios. We consider both latency-sensitive, client/server production applications [35] and bulk-flow, large-scale computation applications [4, 16, 22]. Mixed traffic is considered in Section 6.2.

4.2.1 Latency sensitive services

Web servers and caches within the Facebook datacenter service user requests, where low latency is desirable [43]. Faults harm performance, where either drops or queuing delay can result in unacceptable increases in request latency. Since loss is often a sign of network congestion, the TCP state machine tracks various related statistics. These include the number of retransmitted packets, the congestion window (`cwnd`) and the slow-start threshold (`sstresh`). Latency is also tracked using smoothed round trip time (`srtt`). When considered in isolation, these metrics are limited in usefulness; while a retransmit signifies diminished performance for a flow, it does not provide any predictive power for the underlying cause, or whether a given set of flows experiencing retransmits are doing so for the same underlying reason. Furthermore, while `cwnd` and `ssthresh` decrease with loss, the specific values depend highly on the application pattern. For example, bulk flows tend to have a larger congestion window than mouse flows. Thus, comparing any given flow against an average can be difficult, since it is unclear whether 'worse' performance than average is due to a network issue or traffic characteristics.

However, when augmented with path data, these metrics can become valuable indicators of faults. To illustrate the effectiveness of this approach, we induced a network fault impacting two hosts: one web server, and one cache server. In each case, the local ToR is connected to four aggregation switches. Using `iptables` rules, each host dropped 0.5% of incoming packets that transited the link from the first aggregation switch to the ToR switch. We then measured the TCP metrics for outgoing flows, grouped by which aggregation switch (and, thus, rack downlink) was transited on the way to the host.

Rows 1–6 and 9–14 in Table 1 depict the `cwnd`, `ssthresh`, and retransmission count distributions grouped by inbound downlink for production cache (C) and web servers (W) respectively. While we aggregate the values for the non-faulty links into a single series (the even rows in the table), each individual non-faulty link follows the same aggregate distribution with little variation. On the other hand, the faulty-link distribution for each metric is significantly skewed—towards smaller numbers for `cwnd` and `ssthresh`, and larger for retransmits. Rows 17–22 show that `cwnd`, `ssthresh`, and retransmits provide a similarly strong signal when the link fault impacts traffic in the outbound direction instead. `srtt` is effective for detecting faults that induce latency but not loss; we defer details to Section 5.3.1.

4.2.2 Bulk data processing

Next, we consider bulk data processing workloads. Commonly used frameworks like Hadoop involve reading large volumes of data from various portions of the network; slowdowns caused by the network can have a disproportionate impact on job completion times due to stragglers. While the TCP metrics above work equally well in the case of Hadoop (not shown), the high-volume flows in Hadoop allow us to adopt a higher-level, protocol-independent metric that depends on the buffer dynamics present in any reliable transport protocol.

Consider the case of an application making a blocking system call to send data. Either there will be room present in the connection's network buffer, in which case the data will be buffered immediately, or the buffer does not have enough space and causes the application to wait. As packets are transmitted, the buffer is drained. However, if a fault induces packet drops, packets need to be retransmitted and thus the goodput of the network buffer drops. Correspondingly, the buffer stays full more of the time and the distribution of the latency of `send()` and similar blocking system calls skews larger. Delays caused by packet reordering have similar impacts. Non-blocking sends exhibit this behavior too; we can instrument either the `select()` or `epoll_ctl()` system calls to get insight into buffer behavior.

To demonstrate this, we consider a synthetic traffic pattern representative of the published flow-size distributions for Hadoop workloads present in Facebook's datacenters [35]. Specifically, we designate one server in our testbed (see Section 5.1 for details) as a sink and the remainder as sources. In addition, we induce a random packet drop impacting 1 of 9 testbed core switches. For a fixed period of time, each server in a loop creates a fixed number of simultaneous sender processes. Each sender starts a new flow to the sink, picks a flow size from the Facebook flow-size distribution for Hadoop servers and transmits the flow to completion, while recording the wait times for each `select()` system call.

Rows 23–24 in Table 1 show the distributions of `select()` latencies for flows grouped by core switch transited in our private testbed—again, the non-faulty distributions are aggregated. Faulty links on the impacted core yield a dramatically shifted distribution. Additionally, the distributions for non-faulty cores show little variation (omitted for space). This allows us to differentiate between faulty and normal links and devices. We found the metric to be sensitive to drop rates as low as 0.5%. Moreover, this signal can also be used for caches, due to the long-lived nature of their flows. Rows 7–8 and 15–16 in Table 1 show the distribution of `epoll()` and `select()` latencies for flows on faulty and non-faulty links in production and on the testbed, respectively; in both cases, the faulty link distribution skews larger.

#	Host	Type	Metric	Path	Error	p25	p50	p75	p90	p95	p99
1	(C)	Prod	cwnd	In	0.5%	7 (-30%)	8 (-20%)	10 (par)	10 (par)	10 (-41%)	20 (-33%)
2	(C)	Prod	cwnd	In	-	10	10	10	10	17	30
3	(C)	Prod	ssthresh	In	0.5%	6 (-62.5%)	7 (-63.2%)	18 (-25%)	24 (-64.7%)	31 (-51.6%)	63 (-17.1%)
4	(C)	Prod	ssthresh	In	-	16	19	24	57	64	76
5	(C)	Prod	retx	In	0.5%	0 (par)	1	2	3	4	6
6	(C)	Prod	retx	In	-	0	0	0	0	0	1
7	(C)	Prod	epoll	In	0.5%	0.003 (par)	0.14 (+1.4%)	0.47(+10.8%)	0.71(+30.6%)	1.07 (+60.6%)	2.28 (+125%)
8	(C)	Prod	epoll	In	-	0.003	0.14	0.43	0.54	0.67	1.01
9	(W)	Prod	cwnd	In	0.5%	8 (-63.6%)	12 (-60%)	17 (-74.6%)	38 (-60%)	121 (+23.5%)	139 (-33.2%)
10	(W)	Prod	cwnd	In	-	22	30	67	95	98	208
11	(W)	Prod	ssthresh	In	0.5%	4 (-42.9%)	12 (-40%)	16 (-66.7%)	19 (-75%)	31 (-66.7%)	117 (+19.4%)
12	(W)	Prod	ssthresh	In	-	7	20	48	73	93	98
13	(W)	Prod	retx	In	0.5%	0	0	1	3	4	6
14	(W)	Prod	retx	In	-	0	0	0	0	0	0
15	(C)	Syn	select	Out	2.0%	0.56(+25k%)	4.22(+717%)	7.01(+642%)	37.5(+1.6k%)	216 (+4.3k%)	423 (+969%)
16	(C)	Syn	select	Out	-	0.002	0.516	0.944	2.15	4.90	39.6
17	(W)	Syn	cwnd	Out	0.5%	2 (-80%)	2 (-80%)	2 (-80%)	4 (-60%)	7 (-30%)	10 (par)
18	(W)	Syn	cwnd	Out	-	10	10	10	10	10	10
19	(W)	Syn	ssthresh	Out	0.5%	2 (-50%)	2 (-71%)	2 (-75%)	2 (-78%)	4 (-56%)	7 (-22%)
20	(W)	Syn	ssthresh	Out	-	4	7	8	9	9	9
21	(W)	Syn	retx	Out	0.5	21	23	26	29	30	40
22	(W)	Syn	retx	Out	-	0	0	0	0	0	0
23	(H)	Syn	select	Out	2.0%	22 (+11%)	223 (+723%)	434 (+85%)	838 (+32%)	1244 (+47%)	2410 (+39%)
24	(H)	Syn	select	Out	-	19.5	27.1	235	634	844	1740

Table 1: Metric statistics for Production/Synthetic (C)ache/(W)eb/(H)adoop hosts grouped by (In/Out)bound path and induced loss rates; sycall metrics in msec. Each color-banded pair of rows denotes the base and impacted metrics for (aggregated) working and (unique) faulty paths.

Component	p25	p50	p75	p95
eBPF (paths)	0.17%	0.23%	0.46%	0.65%
TCP metrics/t-test	0.25%	0.27%	0.29%	0.33%

Table 2: End-host monitoring CPU utilization in production.

4.2.3 Metric collection computational overhead

While the aforementioned statistics provide a useful signal, care must be taken when determining how to collect statistics. While system-call latency can be instrumented within an application, that requires potentially invasive code changes. Instead, we again leverage eBPF to track system-call latencies. For TCP statistics, we directly read `netlink` sockets in a manner similar to the `ss` command. Table 2 depicts the overall CPU usage of our TCP statistics collection and verdict generation agent; the cumulative CPU overhead is below 1%.

4.3 Verdict generation

Previously, we demonstrated that path aggregated end-host metrics can single out under-performing groups of flows. Here, we develop an end-host decision engine to generate verdicts based on these metrics.

4.3.1 Outlier detection

Due to the clumping of distributions in the absence of faults, we hypothesize that every observed value of a given metric under test can be treated as a sample from the same underlying distribution characterizing a fault-free link, during a particular time period containing a given load. Moreover, a substantially different distribution applies for a faulty link for the same time period. Thus, determining whether a link is faulty reduces to determining whether the samples collected on that link are part of the same distribution as the fault-free links.

While we cannot state with certainty the parameters of the fault-free distribution due to the complexities of network interactions, we rely on the assumption that the number of faulty datacenter links at any given instant is much lower than the number of working links. Suppose we consider the number of retransmits per flow per link, for all links, over a fixed time period. For each link, we compare its distribution to the aggregate distribution for all the other links. If there exists only one fault in the network, then there are two possible cases: the distribution under consideration is faulty and the aggregate contains samples from exclusively non-faulty links, or it is non-faulty and the aggregate contains samples from 1 faulty link and $(N-1)$ working links. In the former case, the distribution under test is skewed significantly to the right of the aggregate; in the latter, it is skewed slightly to the left (due to the influence of the single faulty link in the aggregate). Thus a boolean classifier can be used: if the test distribution is skewed to the right by a sufficiently large amount, we issue a guilty verdict; else, we do not. Concurrent errors shift the aggregate distribution closer to the outlier distribution for a single faulty link. If every link is faulty, we cannot detect faulty links since we do not find any outliers. However, our method is robust even in the case where 75% of the links have faults; we examine the sensitivity of our approach in Section 5.4.2.

4.3.2 Hypothesis testing

Due to the large volume of traffic, even small time intervals contain a large number of samples. Thus, we have to carefully implement our outlier test to avoid significant end-host computational overhead. Our approach

computes a lightweight statistic for each metric under consideration, for each link, over successive fixed-length (10 seconds by default) sampling periods. Each end host generates verdicts for links associated with its own pod. Thus, for each flow, there are a few tens of possible core-to-aggregation downlinks, and four possible aggregation-to-ToR downlinks. Having acquired TCP metrics and path information for all flows via our collection agent, we bucket each sample for the considered metrics into per-link, per-direction buckets. Thus, each metric is bucketed four times: into the inbound and outbound rack and aggregation (up/down)links traversed.

For TCP retransmit and system-call latency metrics, we compute the t-statistic from the single-tailed 1-sample Student's t-test using a low-overhead and constant-space streaming algorithm. To do so we need the average and standard deviation per distribution, and the aggregate average—all of which are amenable to streaming computation via accumulators, including standard deviation via Welford's Algorithm [41]. We then input the t-statistic to the test. The t-test compares a sample mean to a population mean, rejecting the null hypothesis if the sample mean is larger—in our case, if the tested link has more retransmits or higher system-call latency than the other links in aggregate. In every time period, each host checks if the t-statistic is greater than 0 and the p-value ≤ 0.05. If so, we reject the null hypothesis, considering the link to be faulty.

This approach limits the computational overhead at any individual host since it only needs to track statistics for its own `select()/epoll()` calls and TCP statistics. The bottom row of Table 2 depicts the CPU utilization at a single production web server for this approach over 12 hours. The t-test computation and `netlink` TCP statistics reader uses roughly 0.25% of CPU usage. This result is roughly independent of how often the verdict is computed; the majority of the CPU usage is incrementing the various accumulators that track the components of the t-statistic. The `bcc`/eBPF portion, however, has periods of relatively high CPU usage approaching 1% overall, due to the need to periodically flush fixed-sized kernel structures that track flow data.

For `cwnd`, `ssthresh` and `srtt` TCP statistics, we find the student's t-test to be too sensitive in our environment. However, a modified 2-sample Kolmogorov-Smirnov (KS-2) test provides an effective alternative. Specifically, we compare two down-sampled distributions: the 99-point {p1, p2, ..., p99} empirical distribution for the link under consideration, and a similarly defined distribution for the other links in aggregate.

4.4 Centralized fault localization

While individual hosts can issue verdicts regarding link health, doing so admits significant false positives. Instead, we collate host verdicts at a centralized controller that attempts to filter out individual false positives to arrive at a network-wide consensus on faulty links.

4.4.1 Controller processing

Assuming a reliable but noisy end-host-level signal, we hypothesize that false positives should be evenly distributed amongst links in the absence of faults. Note that while some networks might contain hotspots that skew flow metrics and violate this assumption, traffic in the Facebook datacenter is evenly distributed on the considered timescales, with considerable capacity headroom.

We use a centralized controller to determine if all links have approximately the same number of guilty (or not guilty) verdicts, corresponding to the no-faulty-links case. Hosts write link verdicts—generated once per link every ten seconds—to an existing publish-subscribe (pub-sub) framework used for aggregating log data. The controller reads from the pub-sub feed and counts the number of guilty verdicts per link from all the hosts, over a fixed accumulation period (10 seconds by default). The controller flags a link as faulty if it is a sufficiently large outlier. We use a chi-squared test with the null hypothesis that, in the absence of faults, all links will have relatively similar numbers of hosts that flag it not-guilty. The chi-square test outputs a p-value; if it is ≤ 0.05, we flag the link with the least not-guilty verdicts as faulty. We iteratively run the test on the remaining links to uncover additional faults until there are no more outliers.

4.4.2 Computational overhead

The controller has low CPU overhead: a Python implementation computes 10,000 rounds for tens of links in <1 second on a Xeon E5-2660, and scales linearly in the number of links. Each host generates two verdicts per link (inbound/outbound) every 10 seconds, with O(1000s) hosts per pod. Each verdict consists of two 64-bit doubles (t-stat and p-value) and a link ID. In total, this yields a streaming overhead of < 10 Mbps per pod, well within the capabilities of the pub-sub framework.

5. EVALUATION

We now evaluate our approach within two environments: the Facebook datacenter described in Section 3.1, and a small private testbed. First, we describe our test scenario in each network, and provide a motivating example for real-world fault detection. We then consider the speed, sensitivity, precision, and accuracy of our approach, and conclude with experiences from a small-scale, limited-period deployment at Facebook.

5.1 Test environment

Within one of Facebook's datacenters, we instrumented 86 web servers spread across three racks with the monitoring infrastructure described in Section 4. Path markings are provided by a single Agg switch, which sets DSCP bits based on the core switch from which the packet arrived. (Hence, all experiments are restricted to

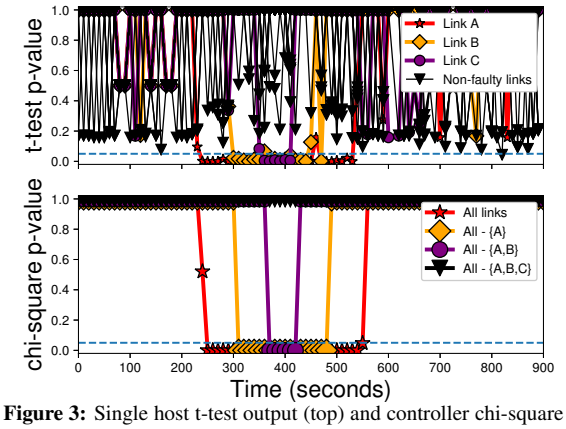

Figure 3: Single host t-test output (top) and controller chi-square output (bottom) for three separate link faults.

the subset of traffic that transits the instrumented Agg switch, and ignores the remainder.) To inject faults, we use `iptables` rules installed at end hosts to selectively drop inbound packets that traversed specific links (according to DSCP markings). For example, we can configure an end host to drop 0.5% of all inbound packets that transited a particular core-to-Agg link. This has the effect of injecting faults at an arbitrary network location, yet impacting only the systems that we monitor.[2]

Our private testbed is a half-populated $k = 6$ fat tree, consisting of 3 (of 6) pods of 9 hosts each, connected via 9 core switches. Each core has three links, one to each pod. To inject faults, we use a 'bump in the wire' to perturb packets on a link. For example, consider a faulty core that drops (or delays) a random subset of packets traversing a link to an Agg. Thus, to inject a fault at that link, we replace the link connecting the core to the Agg with a link connecting it to a network bridge, which is in turn connected to the Agg. The bridge is a Linux host that forwards packets, randomly dropping (or delaying) a subset of packets in a given direction. We implement ECMP using source routing; the 5-tuple therefore allows us to determine the paths packets traverse in our testbed.

5.2 Motivating example

Over a five-minute interval in the Facebook datacenter, we induced faults on links from three different core switches to the instrumented Agg, denoted A, B and C. In particular, we induce faults in the order A, B, C, with a one-minute gap; we then removed the faults in reverse order with the same gap. Each fault is a random 0.5% packet drop (1 in 200 packets). In aggregate, this corresponds to an overall packet loss rate of $< 0.02\%$.

The top portion of Figure 3 depicts the t-test output for a single host. Flows are grouped according to incoming core downlink, and TCP retransmission statistics are aggregated into ten-second intervals. For a single host, for every non-faulty link (every series in black, and the faulty links before/after their respective faults) the t-test output is noisy, with p-values ranging from 0.15 to 1.0. However, during a fault event the p-value drops down to near 0. Close to 100% of the hosts flag the faulty links as guilty, with few false positives.

These guilty verdicts are sent to our controller. The controller runs the chi-squared test every 10 seconds using each core downlink as a category; it counts the number of *non-guilty* verdicts from the end hosts as metric and flags an error condition if the output p-value ≤ 0.05. Note that this flag is binary, indicating that there exists at least one active fault; the guilty verdict count must be consulted to identify the actual guilty link. The bottom portion of Figure 3 depicts the controller output using this mechanism. We depict the output of the test for all paths (in red), and for the set of paths excluding faulty paths $\{A\}$, $\{A, B\}$ and $\{A, B, C\}$ (in yellow, purple and black, respectively). These results indicate that the controller will flag the presence of a fault as long as there is at least one faulty link in the set of paths under consideration, thus supporting an iterative approach.

5.3 Speed and sensitivity

For our mechanism to be useful, it must be able to rapidly detect faults, even if the impact is slight. Moreover, ideally we could detect faults that result in increased latency, not just those that cause packet loss.

5.3.1 *Loss rate sensitivity*

We performed a sensitivity analysis on the amount of packet loss we can detect in the datacenter. While loss rates $\geq 0.5\%$ are caught by over 90% of hosts, we see a linear decrease in the number of guilty verdicts as the loss decreases past that point—at 0.1% drop rate, only $\approx 25\%$ of hosts detect a fault in any given 10-second interval, reducing our controller's effectiveness. However, we can account for this by prolonging the interval of the controller chi-square test. Figure 4a depicts the distribution of p-values outputted by the controller for a given loss rate and calculation interval. Each point with error bars depicts the median, p5 and p95 p-values outputted by the controller during a fault occurrence; each loss rate corresponds to a single series. We see that while a 0.25% loss is reliably caught with a 20-second interval, a 0.15% loss requires 40 seconds to be reliably captured; lower loss rates either take an unreasonably large (more than a minute) period of time to be caught or do not get detected at all. Note that in the no-fault case, no false positives are raised despite the increased monitoring interval.

5.3.2 *High latency detection*

In our private testbed, we induced delays for traffic traversing a particular core switch. To do this, we used Linux `tc-netem` on our 'bump-in-the-wire' network bridges to add constant delay varying from 100

[2]Note that while all monitored hosts will see the same loss *rate* across the link, the actual packets dropped may vary because `iptables` functions independently at each host.

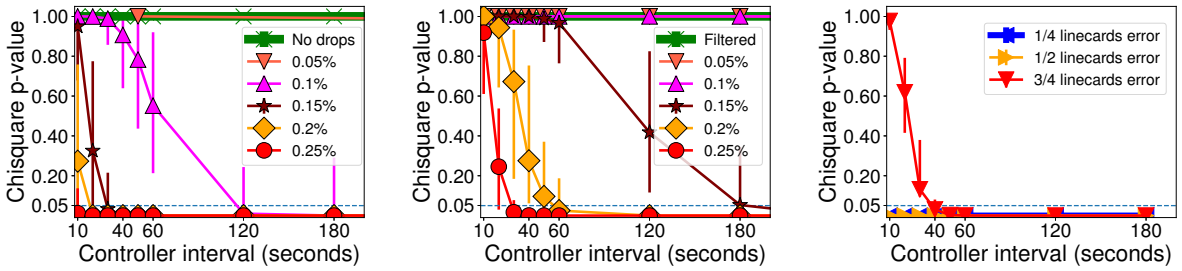

(a) Single fault loss rate sensitivity. **(b)** Masked fault sensitivity. **(c)** Linecard faults.

Figure 4: Controller chi-square p-value convergence for various faults vs. controller interval length.

Request bytes	Latency msec	p50	p75	p95	p99
100	-	1643	1680	2369	2476
100	0.1	3197	3271	4745	4818
100	1.0	10400	10441	19077	19186
8000	-	4140	4778	619	7424
8000	0.1	6809	7510	9172	11754
8000	0.5	11720	14024	18367	21198

Table 3: `srtt_us` distribution vs. additional latency and request size. The no-additional-latency case is aggregated across all non-impacted links, while the others correspond to a single (faulty) link.

microseconds to 1 millisecond (a typical 4-MB switch buffer at 10 Gbps can incur a maximum packet latency of roughly 3 milliseconds before overflowing). We then ran client/server traffic with a single pod of 9 HHVM [5] servers serving static pages, and two pods (18 hosts) configured as web clients running Apache Benchmark [1]. Each server handled 180 simultaneous clients and served either small (100-B) or medium (8-KB) requests.

Table 3 depicts the distributions for TCP `srtt_us` TCP at a particular end host as a function of induced latency and request size. As in previous experiments, the distributions of non-impacted links are very close to each other, while the distribution of the latency heavy link is clearly differentiable. No drops were detected in the 100-B case; due to our use of 1-Gbps links, a handful of drops comparable to the no-fault case were detected in the 8-KB case. The modified KS-2 test operating over a 10-second interval correctly flags all intervals experiencing a latency increase, while avoiding false positives.

5.4 Precision and accuracy

Next, we demonstrate the precision and accuracy of the system in the presence of concurrent and correlated faults, as well as the absence of false positives.

5.4.1 Concurrent unequal faults

A large network will likely suffer concurrent faults of unequal magnitude, where the largest fault may mask the presence of others. While we surmise that the most visible fault will be easily diagnosable, ideally it would be possible to parallelize fault identification in this case.

We consider a scenario in the Facebook datacenter with two concurrent faults on distinct core-to-Agg switch links: one causing a packet loss rate of 0.5%, and one with a rate that varies from 0.25% to 0.15% (which we can easily identify in isolation). Using TCP retransmit statistics, the high-loss fault was flagged by almost all the hosts the entire time, while the flagging rate for the lower-impact fault depends roughly linearly on its magnitude. However, the drop-off in guilty verdicts is steeper in the presence of a masking, higher-impact fault. As a result, the 10- and 20-second controller intervals that flag the low-loss-rate faults in isolation no longer suffice.

Figure 4b depicts the controller chi-square p-value outputs for the set of paths *excluding* the one suffering from the readily identified larger fault; each series corresponds to a different loss rate for the smaller fault. The interval needed to detect such "masked" faults is longer; a 0.25% loss rate requires a 40-second interval to reliably be captured vs. 20 seconds in the unmasked case (Figure 4a), while a 0.15% rate requires over three minutes.

5.4.2 Large correlated faults

So far, we have considered faults impacting a small number of uncorrelated links. However, a single hardware fault can affect multiple links. For example, each Agg switch contains several core-facing linecards, each providing a subset of the switch's cross-pod capacity. A linecard-level fault would thus affect several uplinks. Similarly, a ToR-to-Agg switch link might be impacted, affecting a full quarter of the uplinks for that rack's hosts. Our approach relies on the student's t-test picking outliers from a given average, with the assumption that the average represents a non-broken link. However, certain faults might impact a vast swath of links, driving the average performance closer to that of the impacted links'.

To test this scenario, we induce linecard-level faults on 25%, 50%, 75% and 100% of the uplinks on the instrumented Agg switch in the Facebook datacenter. The per-link loss rate in each case was 0.25%. With 100% faulty links, our method finds no faults since no link is an outlier—a natural consequence of our approach. How-

Metric	Error	p50	p90	p95	p99
retx	-	0	0	1	2
retx	0.5%	1	3	4	5
cwnd	-	10	18	26	39
cwnd	0.5%	9	10	16	28

Table 4: TCP congestion window and retransmit distributions when binning by remote rack with a faulty rack inducing a 0.5% drop rate.

ever, in all other cases our approach works if the hosts declare paths faulty when the p-value ≤ 0.1. Figure 4c shows the controller performance for various linecard-level faults as a function of interval length. A 10-second interval captures the case where 25% of uplinks experience correlated issues, but intervals of 20 and 40 seconds, respectively are required in the 50% and 75% cases.

5.4.3 *False positives*

The longer our controller interval, the more sensitive we are to catching low-impact faults but the more likely we are to be subject to false positives. We ran our system in production in the absence of any (known) faults with intervals ranging from 10 seconds to an hour. Even with 30-minute intervals, the lowest p-value over 42 hours of data is 0.84; only one-hour intervals generated any false positives ($p \leq 0.05$) in our data. We note, however, that we need not support arbitrarily large intervals. Recall that an interval of roughly three minutes is enough to get at least an intermittent fault signal for a 0.1% loss rate.

5.4.4 *Granular faults and alternative binnings*

By default, our approach bins flow metrics by path. In certain cases, however, a fault may only impact a specific subset of traffic. For example, traffic from a particular subnet might exhibit microburst characteristics, periodically overflowing switch buffers and losing packets.

Alternative binnings can be employed to identify such "granular" faults. To illustrate, we induced a fault at a single cache server, in which packets from exactly one remote rack are dropped at a rate of 0.5%. We then binned traffic by remote rack. Table 4 depicts the distribution of congestion window and retransmit by remote rack; as before, the distributions for non-impacted bins are all close to each other. The KS-2 test and t-test successfully pick out the fault without false positives using the `cwnd` and retransmissions metrics respectively. Note such alternative binning can help diagnose faults even if there is no path diversity—in this case, the alternatives are provided by application load balancing.

5.5 Small-scale deployment experience

While our experiments focus on injected failures, we are obviously interested in determining whether our system can successfully detect and localize network anomalies "in the wild". Thus, we examine the performance of our system over a relatively long time period (in the absence of any induced failures) to answer the following questions: "Does our system detect performance anomalies?" "Do non-issues trigger false positives?" "Do we notice anomalies before or after Facebook's existing fault-detection services catch it?"

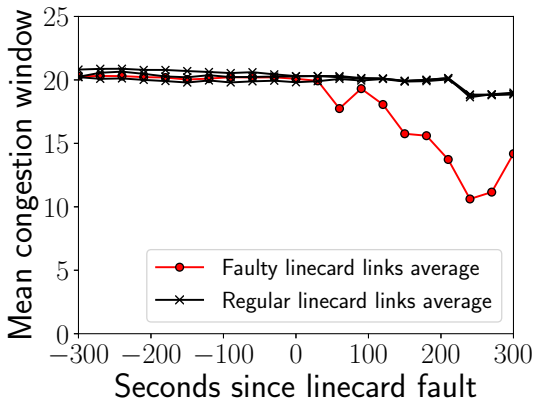

Figure 5: Mean `cwnd` per (host,link) during linecard fault.

To answer these questions, we deployed our system on 30 hosts for a two-week period in early 2017. As an experimental system, deployment was necessarily restricted; our limited detection surface thus impacted our chance of detecting partial faults. An operator of another large-scale datacenter suggests that, in their experience, partial failures occur at a rate of roughly 10 per day in a network containing O(1M) hosts [28]. It is not surprising, then, that our two-week trial on only 30 hosts did not uncover any partial faults. We were, however, able to derive useful operational experience that we relate below.

5.5.1 *Response to organic failure*

On January 25th, 2017, the software agent managing a switch linecard that our system was monitoring failed. The failure had no immediate impact on traffic; the data-plane continued to forward traffic according to the most recent ruleset installed by the agent. Thus, the initial failure is invisible to and explicitly outside the scope of our tool, which focuses only on faults that impact traffic.

Roughly a minute later, however, as the BGP peerings between the linecard and its neighbors began to time out, traffic was preemptively routed away from the impacted linecard. Thus, applications saw no disruption in service despite the unresponsive linecard control plane. Yet, we observe that as traffic was routed away from the failed linecard, the distributions of TCP's `cwnd` and `ssthresh` metrics for the traffic remaining on the linecard's links rapidly diverged from the values on other links in the equivalence set. Figure 5 depicts the per-link mean congestion window measured by every host, aggregated per-linecard and averaged across every corresponding host, with the afflicted linecard colored red.

The deviations are immediate and significant, with the mean `cwnd` dropping over 10% in the first interval after

the majority of traffic is routed away, and continually diverging from the working links thereafter. Furthermore, the volume of measured flows at each host traversing the afflicted linecard rapidly drops from O(1000s) to O(10s) per link. By contrast, one of Facebook's monitoring systems, NetNORAD [6], took several minutes to detect the unresponsive linecard control plane and raise an alert.

It is important to note that in this case, we did not catch the underlying software fault ourselves; that honor goes to BGP timeouts. However, we do observe a sudden shift in TCP statistics in real time as traffic is routed away, as our system was designed to do. With respect to our stated goal—to pinpoint the links responsible for deleterious traffic impact—our system performs as expected. Thus, this anecdote shows that our system can compliment existing fault-detection systems, and provide rapid notification of significant changes in network conditions on a per-link or per-device basis.

5.5.2 Filtering normal congestion events

During the monitoring period, no other faults were detected by the system. While a small number of false positives were generated in every interval, the controller filters out these indications since the noise is spread across the monitored links. However, we noticed that the number of false positives had periodic local maxima around 1200 and 1700 GMT. Furthermore, these were correlated with the raw (i.e., independent of flow/path) TCP retransmit counts tracked by the end hosts. Given that they occurred at similar times each day and were evenly spread across all the monitored hosts, we surmise that these retransmits were not due to network faults, but organically occurring congestion. This experience provides some confidence that our system effectively distinguishes between transient congestion and partial faults.

6. APPLICABILITY

Here, we consider the applicability of our approach in various challenging scenarios, e.g., datacenters with heterogeneous traffic patterns, topologies less amenable to single-marking path discovery (either by design or due to failed links re-routing traffic), virtualized multi-tenant environments, and more. We first list some conditions to which our approach is resilient. Subsequently, we clarify the extent to which traffic homogeneity, link failures and topology impact the suitability of our approach. We conclude with a discussion on known limitations.

6.1 Surmountable issues

While we have access to only one production environment, we have conducted sensitivity analyses in our testbed to consider alternative deployments. Due to space limits, we summarize our findings here, but provide more extensive discussion in Appendix B.

1. **VMs and high CPU utilization**: Our datacenter tests were on bare metal; we find the approach works equally well in a hypervisor-based environment, even when the hardware CPU is fully taxed.
2. **Mixed, over-subscribed and uneven traffic**: The Facebook datacenter lacks saturated links and uneven load. We consider a mixed workload with latency sensitive and core-saturating bulk traffic, where server load ranges from $1\times$—$16\times$.
3. **TCP settings**: Datacenter hosts employ NIC offload features such as TSO. Turning these optimizations off does not obscure TCP or timing-based signals; neither does varying buffer sizes across three orders of magnitude (16 MB—16 KB).

6.2 Traffic homogeneity

Facebook traffic is highly load balanced [35], aiding our outlier-based detection approach. We are optimistic, however, that our method is also applicable to datacenters with more heterogeneous and variable workloads. That said, outlier analysis is unlikely to succeed in the presence of heterogeneous traffic if we do not carefully pick the links or switches that we compare against each other—specifically, if we fail to form a valid ES.

In the case of our experiments at Facebook, the ES we used was the set of downlinks from the network core into a pod. ECMP routing ensured that these links did form an ES; all cross-pod flows had an equal chance of mapping to any of these links, and the path from these links down to the hosts were equal cost. This characteristic notably holds true regardless of the specific mix of traffic present. Thus, we hypothesize that on any network where such an ES can be formed, our approach works regardless of traffic homogeneity. To demonstrate this, we ran our fat-tree testbed with a worst case scenario of heterogeneous traffic: running synthetic bulk transfer and latency sensitive RPC traffic, with heavy traffic skew (with per host-load ranging from 1–16$\times$ the minimum load). Furthermore, we overloaded the network core by artificially reducing the number of links. Even in this case, our t-test classifier operating on the `select()` latency metric was able to successfully differentiate the outlier link.

6.3 Link failures

In addition to being able to detect and localize partial faults, our system must be able to account for total link failures, which can confound our ability to determine a flow's path through the network due to re-routing. Consider the outcome of a total link failure on the fate of traffic routed via that link. There are three possible outcomes for such traffic: (1) traffic is redirected at a prior hop to a working alternative path, (2) traffic is re-routed by the switch containing the dead-end link to a backup non-shortest path, and (3) traffic is black holed and the flow stops (the application layer might restart the flow).

Cases (1) and (3) do not affect our approach. ECMP routing will ensure that flows are evenly distributed among the surviving links, which still form an ES (al-

beit one smaller in size than before the failure). Case (2) can impact our approach in two ways. First, traffic taking a longer path will likely see worse performance compared to the rest of the traffic that traverses links on the backup path—harming the average performance on that path. Moreover, backup path performance might drop due to unfair loading as more flows join. Presuming rerouting is not silent (e.g., because it is effected by BGP), the former effect can be accounted for; traffic using backup routes can be marked by switches and ignored in the end-host t-test computation. The latter can be mitigated by careful design: rather than loading a single backup path unfairly, the load can be evenly distributed in the rest of the pod. Even if an imbalance cannot be avoided, two smaller ESes can yet be formed: one with links handling rerouted traffic, and one without.

6.4 Topologies

Our system leverages the details of Facebook's datacenter topology to obtain full path info with a single marking identifying the transited core switch. The topology also allows us to form equivalence sets for each pod by considering the core-to-pod downlinks. Other networks might provide more challenging environments (e.g. middleboxes or software load balancers [31] might redirect some traffic; different pods might have varying internal layouts; links might fail) that confound the ability to form equivalence sets. In an extreme case, a Jellyfish-like topology [38] might make it extremely difficult to both extract path information and form ESes.

In certain cases, though, even networks with unruly layouts and routing can be analyzed by our approach. Consider a hybrid network consisting of a Jellyfish-like subset. For example, suppose a single switch in the Jellyfish sub-network is connected to every core switch in a multi-rooted tree, with identical link bandwidths. While we cannot reason about traffic internal to the Jellyfish, we can still form an ES for the links from the single switch connecting to the regular topology, for all traffic flowing into the regular sub-network. No matter how chaotic the situation inside the Jellyfish network, the traffic should be evenly distributed across core switches in the regular sub-network, and from then on the paths are equivalent.

Note that here, we only consider the subset of the path that lies within the regular topology. As long as an ES can be formed, the path behind it can be considered as a black box. Thus, we argue that even on topologies where we can't find the full path, or where inequalities in path cost exist, we can run our approach on subsets of the topology where our requirements do hold.

6.5 Limitations

On the other hand, there are certain cases where our current approach falls short. To begin, we presume we are able to collect end-host metrics that reflect network performance. While we believe our current metrics cover the vast majority of existing deployments, we have not yet explored RDMA-based applications or datacenter fabrics. Our current metrics also have limits to their precision; while we can detect 0.1% drop rates in the datacenter we studied, past a certain point we are unable to discern faults from noise. Moreover, the production datacenter is well provisioned, so fault-free performance is stable, even in the tail. Hence, we do not consider the inability to detect minor impairments to be a critical flaw: If the impacts of a fault are statistically indistinguishable from background network behavior, then the severity of the error might not be critical enough to warrant immediate response. Datacenters operating closer to capacity, however, may both exhibit less stable fault-free behavior, as well as require greater fault-detection sensitivity.

Despite extensive use of ECMP and application load-balancing techniques, datacenter networks with mixed workloads may include links that see more traffic and congestion than others. That said, we have not encountered enough variability in load in the network core and aggregation layers to trigger enough false positives to confound the accuracy of our method in either production or under our testbed, and thus cannot yet quantify under what circumstances this degradation in detection performance would occur. Furthermore, for links lacking alternatives—such as an end host to top-of-rack access link in the absence of multihoming—we cannot pick out an outlier by definition since there is only one link to analyze. We can, however, still perform our analysis on different groupings within traffic for that link; for example, when traffic to a particular subnet is impacted.

7. SUMMARY

We have demonstrated a method to use the regularity inherent in a real-world deployment to help rapidly detect and localize the effects of failures in a production datacenter network. In particular, we have shown that we can do it with reasonable computational overhead and ease of deployment. We believe improvements in network core visibility, together with coordinating end-host performance monitoring with centralized network control, can aid the task of managing network reliability.

ACKNOWLEDGMENTS

This work is supported in part by the National Science Foundation through grants CNS-1422240 and CNS-1564185. We are indebted to Aaron Schulman, Ariana Mirian, Danny Huang, Sunjay Cauligi, our shepherd, Dave Maltz, and the anonymous reviewers for their feedback. Alex Eckert, Alexei Starovoitov, Daniel Neiter, Hany Morsy, Jimmy Williams, Nick Davies, Petr Lapukhov and Yuliy Pisetsky provided invaluable insight into the inner workings of Facebook services. Finally, we thank Omar Baldonado for his continuing support.

8. REFERENCES

[1] ab - Apache HTTP server benchmarking tool. https://httpd.apache.org/docs/2.4/programs/ab.html.

[2] BPF Compiler Collection (BCC). https://github.com/iovisor/bcc/.

[3] Extending extended BPF. https://lwn.net/Articles/603983/.

[4] Hadoop. http://hadoop.apache.org/.

[5] HHVM. http://hhvm.com.

[6] A. Adams, P. Lapukhov, and H. Zeng. https://code.facebook.com/posts/1534350660228025/netnorad-troubleshooting-networks-via-end-to-end-probing/.

[7] M. Aguilera, J. Mogul, J. Wiener, P. Reynolds, and A. Muthitacharoen. Performance Debugging for Distributed Systems of Black Boxes. SOSP, Bolton Landing, NY, USA, 2003. ACM.

[8] M. Al-Fares, A. Loukissas, and A. Vahdat. A Scalable, Commodity Data Center Network Architecture. SIGCOMM, Seattle, WA, USA, 2008. ACM.

[9] A. Andreyev. Introducing data center fabric, the next-generation Facebook data center network. https://code.facebook.com/posts/360346274145943, 2014.

[10] B. Arzani, S. Ciraci, B. T. Loo, A. Schuster, and G. Outhred. Taking the Blame Game out of Data Centers Operations with NetPoirot. SIGCOMM, Florianopolis, Brazil, 2016. ACM.

[11] P. Bahl, R. Chandra, A. Greenberg, S. Kandula, D. A. Maltz, and M. Zhang. Towards Highly Reliable Enterprise Network Services via Inference of Multi-level Dependencies. SIGCOMM, Kyoto, Japan, 2007. ACM.

[12] D. Banerjee, V. Madduri, and M. Srivatsa. A Framework for Distributed Monitoring and Root Cause Analysis for Large IP Networks. SRDS, Niagara Falls, NY, USA, 2009. IEEE Computer Society.

[13] M. Y. Chen, A. Accardi, E. Kiciman, J. Lloyd, D. Patterson, A. Fox, and E. Brewer. Path-based Faliure and Evolution Management. NSDI, San Francisco, California, 2004. USENIX Association.

[14] M. Y. Chen, E. Kiciman, E. Fratkin, A. Fox, and E. Brewer. Pinpoint: Problem Determination in Large, Dynamic Internet Services. DSN, Bethesda, MD, USA, 2002. IEEE Computer Society.

[15] Cisco. BGP Support for TTL Security Check. http://www.cisco.com/c/en/us/td/docs/ios/12_2s/feature/guide/fs_btsh.html.

[16] J. Dean and S. Ghemawat. MapReduce: Simplified Data Processing on Large Clusters. OSDI, San Francisco, CA, 2004. USENIX Association.

[17] N. Duffield, F. L. Presti, V. Paxson, and D. Towsley. Network Loss Tomography Using Striped Unicast Probes. *ACM Transactions on Networking*, 14(4), Aug. 2006.

[18] G. Forman, M. Jain, M. Mansouri-Samani, J. Martinka, and A. C. Snoeren. Automated Whole-System Diagnosis of Distributed Services Using Model-Based Reasoning. DSOM, Newark, DE, Oct. 1998.

[19] C. Guo, L. Yuan, D. Xiang, Y. Dang, R. Huang, D. Maltz, Z. Liu, V. Wang, B. Pang, H. Chen, Z.-W. Lin, and V. Kurien. Pingmesh: A Large-Scale System for Data Center Network Latency Measurement and Analysis. SIGCOMM, London, United Kingdom, 2015. ACM.

[20] N. Handigol, B. Heller, V. Jeyakumar, D. Mazières, and N. McKeown. I Know What Your Packet Did Last Hop: Using Packet Histories to Troubleshoot Networks. NSDI, Seattle, WA, 2014. USENIX Association.

[21] T. Hoff. Latency Is Everywhere And It Costs You Sales - How To Crush It. http://highscalability.com/latency-everywhere-and-it-costs-you-sales-how-crush-it.

[22] M. Isard, M. Budiu, Y. Yu, A. Birrell, and D. Fetterly. Dryad: Distributed Data-parallel Programs from Sequential Building Blocks. EuroSys, Lisbon, Portugal, 2007. ACM.

[23] A. Kabbani, B. Vamanan, J. Hasan, and F. Duchene. FlowBender: Flow-level Adaptive Routing for Improved Latency and Throughput in Datacenter Networks. CoNEXT, Sydney, Australia, 2014. ACM.

[24] S. Kandula, D. Katabi, and J.-P. Vasseur. Shrink: A Tool for Failure Diagnosis in IP Networks. MineNet, Philadelphia, Pennsylvania, USA, 2005. ACM.

[25] R. R. Kompella, J. Yates, A. Greenberg, and A. C. Snoeren. IP Fault Localization via Risk Modeling. NSDI, Boston, MA, USA, 2005. USENIX Association.

[26] R. R. Kompella, J. Yates, A. Greenberg, and A. C. Snoeren. Detection and Localization of Network Black Holes. INFOCOM, Anchorage, AK, USA, 2007. IEEE Computer Society.

[27] R. R. Kompella, J. Yates, A. Greenberg, and A. C. Snoeren. Fault Localization via Risk Modeling. *IEEE Trans. Dependable Secur. Comput.*, 7(4), Oct. 2010.

[28] D. Maltz. Private communication, Feb. 2017.

[29] V. Mann, A. Vishnoi, and S. Bidkar. Living on the edge: Monitoring network flows at the edge in cloud data centers. COMSNETS, Bangalore, India, 2013. IEEE.

[30] R. N. Mysore, R. Mahajan, A. Vahdat, and G. Varghese. Gestalt: Fast, Unified Fault Localization for Networked Systems. USENIX ATC, Philadelphia, PA, 2014. USENIX Association.

[31] P. Patel, D. Bansal, L. Yuan, A. Murthy, A. Greenberg, D. A. Maltz, R. Kern, H. Kumar, M. Zikos, H. Wu, C. Kim, and N. Karri. Ananta: Cloud Scale Load Balancing. SIGCOMM, Hong Kong, China, 2013. ACM.

[32] S. Radhakrishnan, M. Tewari, R. Kapoor, G. Porter, and A. Vahdat. Dahu: Commodity Switches for Direct Connect Data Center Networks. ANCS, San Jose, California, USA, 2013. IEEE Press.

[33] P. Reynolds, J. L. Wiener, J. C. Mogul, M. K. Aguilera, and A. Vahdat. WAP5: Black-box Performance Debugging for Wide-area Systems. WWW, Edinburgh, Scotland, 2006. ACM.

[34] M. Roughan, T. Griffin, Z. M. Mao, A. Greenberg, and B. Freeman. IP Forwarding Anomalies and Improving Their Detection Using Multiple Data Sources. NetT, Portland, Oregon, USA, 2004. ACM.

[35] A. Roy, H. Zeng, J. Bagga, G. Porter, and A. C. Snoeren. Inside the Social Network's (Datacenter) Network. SIGCOMM, London, United Kingdom, 2015. ACM.

[36] S. Savage, D. Wetherall, A. Karlin, and T. Anderson. Practical Network Support for IP Traceback. SIGCOMM, Stockholm, Sweden, 2000. ACM.

[37] A. Singh, J. Ong, A. Agarwal, G. Anderson, A. Armistead, R. Bannon, S. Boving, G. Desai, B. Felderman, P. Germano, A. Kanagala, J. Provost, J. Simmons, E. Tanda, J. Wanderer, U. Hölzle, S. Stuart, and A. Vahdat. Jupiter Rising: A Decade of Clos Topologies and Centralized Control in Google's Datacenter Network. SIGCOMM, London, United Kingdom, 2015. ACM.

[38] A. Singla, C.-Y. Hong, L. Popa, and P. B. Godfrey. Jellyfish: Networking Data Centers Randomly. NSDI, San Jose, CA, 2012. USENIX Association.

[39] D. Turner, K. Levchenko, J. C. Mogul, S. Savage, and A. C. Snoeren. On Failure in Managed Enterprise Networks. Technical report, Hewlett-Packard Labs, May 2012.

[40] D. Turner, K. Levchenko, A. C. Snoeren, and S. Savage. California Fault Lines: Understanding the Causes and Impact of Network Failures. SIGCOMM, New Delhi, India, 2010. ACM.

[41] B. P. Welford. Note on a Method for Calculating Corrected Sums of Squares and Products. *Technometrics*, 4(3), 1962.

[42] X. Wu, D. Turner, C.-C. Chen, D. A. Maltz, X. Yang, L. Yuan, and M. Zhang. NetPilot: Automating Datacenter Network Failure Mitigation. SIGCOMM, Helsinki, Finland, 2012. ACM.

[43] D. Zats, T. Das, P. Mohan, D. Borthakur, and R. Katz. DeTail: Reducing the Flow Completion Time Tail in Datacenter Networks. SIGCOMM, Helsinki, Finland, 2012. ACM.

[44] Y. Zhu, N. Kang, J. Cao, A. Greenberg, G. Lu, R. Mahajan, D. Maltz, L. Yuan, M. Zhang, B. Y. Zhao, and H. Zheng. Packet-Level Telemetry in Large Datacenter Networks. SIGCOMM, London, United Kingdom, 2015. ACM.

A. ALTERNATIVE METHODS

Alternative methods abound for investigating datacenter faults. One appealing option is to couple switch counters with programmable switches. For example, suppose a switch is configured such that when a packet is dropped, either due to error or queuing pressure, it is probabilistically sampled to the switch CPU (note that with switches shifting millions of packets a second, examining all packets leads to unacceptable CPU overhead). Additionally, some switches can be configured to sample packets from high occupancy queues. Thus, counters could indicate a fault, while sampled packets could be used to build a picture of which traffic is impacted.

While this method can alert network operators to faulty links, it is slow in determining which traffic is impacted. Suppose a link carrying 2,000,000 packets per second develops a 0.5% drop rate, leading to 10,000 drops per second. Such a link might be carrying tens of thousands of flows, however. With a relatively high 1 in 100 sampling rate (and thus, 100 sampled packets per second), and with just 10,000 flows carried (a large underestimation) it would take around 100 seconds to determine all the flows if the sampling was perfect and captured a different 5-tuple each time. Furthermore, this would be subject to sampling bias; a lightweight flow carrying control traffic might lose packets but fly under the radar of sampled dropped packets. One heavy handed potential approach could be to disable the entire link; however, consider the case of a partial fault only affecting a subset of traffic (for example, a misconfigured routing rule). In such a case, disabling the entire link would penalize all traffic routed through that link without providing any insight to the underlying problem.

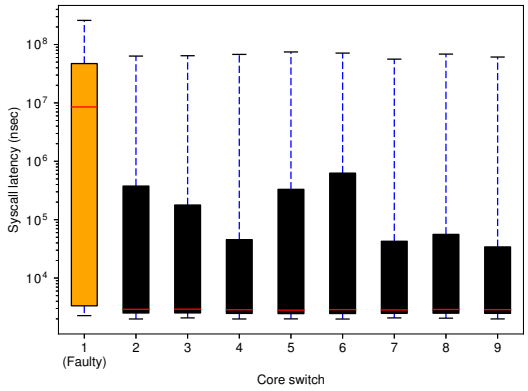

Figure 6: `select()` latency distribution per core switch for the two-VM CPU stress test.

For contrast, our proposed system can quickly identify all the flows impacted by a link error in a less than a minute in several tested cases. In the case of granular errors affecting only a subset of traffic (by source or destination subnet, application port, queuing policy, etc.) our mechanism can still detect outliers, enabling end hosts to reroute around damaged links for afflicted traffic as a stopgap measure. Note that switch counters can be used in conjunction with our methods; features of sampled dropped or latency enduring packets could be used to guide our system's binning of flows in order to converge on which traffic is affected by link faults even quicker. Furthermore, our proposed system is ASIC agnostic since we do not rely on the features of any given chipset. Finally, it is robust to unreliable reporting by switches, as well as the uncertainty of counters that might arise within environments using cut-through routing.

B. METRIC ROBUSTNESS

Here, we demonstrate the effectiveness of our approach in the presence of pathological confounding factors. These experiments are performed on our private testbed, since we could not induce harmful configuration changes in production traffic. We focus on syscall latency metrics, which are less obviously robust to many of thse factors. To save space, we omit similarly strong results using TCP statistics.

B.1 CPU utilization

Datacenter networks run a variety of applications, frequently with stringent CPU requirements and high utilization. To be general, our approach needs to cope with high utilization figures. Furthermore, while some datacenters run applications on bare metal hardware, a significant number of installations use virtual machines.

In order to ascertain the impact of virtual machine hardware and high cpu utilization on our approach, we set up an experiment where each host in our private testbed runs two virtual machines, `cpuvm` and `netvm`. Each instance of `cpuvm` runs a variety of simultaneous CPU intensive tasks: specifically, a fully loaded `mysql` server instance (with multiple local clients), a scheduler-intensive multithreading benchmark, and an ALU-operation-intensive math benchmark. This causes the CPU utilization of the bare metal host to go to 100%. Meanwhile, each instance of `netvm` runs a bidirectional client-server communication pattern using flow size distributions prevalent in certain datacenters [35]. This situation is analogous to the case where one VM is shuffling data for a map-reduce job, while another is actively processing information, for example. Figure 6 depicts the distribution of `select()` latencies across each core switch in the presence of this extreme CPU stress. The distribution corresponding with paths through the faulty switch are clearly distinguishable, with a median value over three orders of magnitude greater than the no-error case. This corresponds to a 100% accuracy rate of flagging the faulty link using our chi-squared test over 1-minute intervals for a 5-minute long test.

B.2 Oversubscription and uneven load

Thus far, all our experiments have networks without saturated core links. While this is a desirable quality in real deployments, it might not be feasible depending on the amount of oversubscription built into the network. Furthermore, in heterogeneous environments such as multi-tenant datacenters, it is conceivable that not every end-host is participating in monitoring traffic metrics. Finally, not every system that is being monitored is subject the same load.

To determine how our approach deals with these challenges, we devised an experiment in our private testbed where 1/3rd of our 27 hosts are no longer participating in monitoring. Instead, these hosts suffuse the network with a large amount of background traffic, with each so-called 'background host' communicating with all other background hosts. Each background host sends a large amount of bulk traffic; either rate limited to a fraction of access link capacity, or unbound and limited only by link capacity. In conjunction with this, our network core is reduced to 1/3rd of normal capacity: from 9 core switches to 3. Thus, the background hosts can, by themselves, saturate core capacity. Our remaining 18 servers continue to run the bidirectional client-server network pattern, with one important difference: rather than all servers having the same amount of load, they are partitioned into three classes. The first class chooses flow sizes from the Facebook cache server flow size distribution [35]; the other two classes choose flow sizes from larger $4\times$ and $16\times$ multiples of the Facebook distribution. In other words, the $4\times$ distribution is simply the normal distribution, except every value for flow size being multiplied by 4.

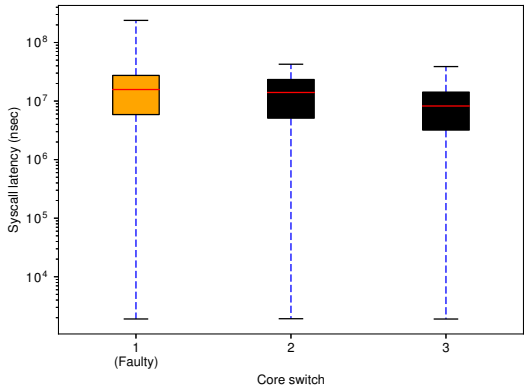

Figure 7: `select()` latency distribution per core switch for the oversubscribed background traffic uneven server test.

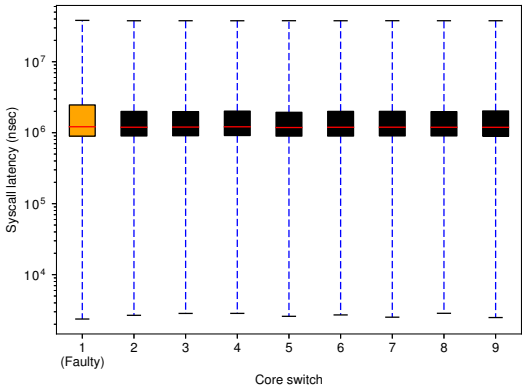

Figure 8: `select()` latency distribution per core switch for the 10-Gbps 16-KB socket send buffer test.

Thus, the link utilizations of the $4\times$ and $16\times$ distributions are correspondingly higher than normal. While the normal distribution has a link utilization of roughly 100 Mbps in this case, the $4\times$ case and $16\times$ cases bring us to roughly 40% and 100% link utilization respectively.

Figure 7 depicts the `select()` latency distribution for this scenario as a multi-series CDF. Each series represents the distribution for a single network path; there is one faulty path and two working paths in this case. The x-axis depicts latency in nanoseconds. Despite the combination of confounding factors, the distribution for the faulty path remains significantly higher (shifted to the right in the figure) than the non-faulty paths (which possess roughly equivalent distributions). Correspondingly, the signal derived from the select() latencies remains useful. Using 1-minute intervals, we note that the chi-squared test hovered at close to 0 when we considered all paths, and close to 1 when the faulty path was removed from the set of candidate paths. This indicates that we remain successful at finding the faulty link even under these circumstances.

B.3 Sensitivity to TCP send buffer size

Our system call latency approach uses the latency of `select()`/`epoll()` calls by hosts that are sending data over the network as a signal. As a reminder, when an application calls `select()`/`epoll()` (or `send()`) on a socket, the call returns (or successfully sends data) when there is enough room in the per-flow socket buffer to store the data being sent. Thus, the distribution of results is fundamentally impacted by the size of the per-flow socket buffer. Note that with the advent of send-side autotuning in modern operating systems, the size of this buffer is not static. In Linux, the kernel is configured with a minimum size, a default (initial) size and a maximum size, with the size growing and shrinking as necessary.

By default, our private testbed systems are configured with a maximum send buffer size of 4 MB. Values for the median buffer size vary from 1.5–2.5 MB for our server hosts and 0.8–1.2 MB for our client hosts in our bidirectional traffic pattern. To determine the sensitivity of our approach to buffer size, we first increased the buffer size to values of 8 and 16 MB. Then, we decreased the buffer size significantly, to values of 52, 26 and 16 KB (note that 16 KB is the default initial size). We noticed that TCP autotune prevents the buffer from growing too large even if the maximum is set significantly higher than default; accordingly, raising the maximum had little to no impact.

Reducing the maximum buffer size, however, is expected to have a larger impact on our metrics. Intuitively, a smaller buffer should correspond with higher overall buffer occupancy; thus, a larger percentage of `select()` and `send()` calls would need to wait until the buffer is drained. This should have the two-fold effect of shifting the `select()` latency distributions to the right—since more calls to `select()` wait for longer—and decreasing the distance between a faulty-path distribution and the normal case.

To test this out, we ran our bidirectional client-server traffic pattern using 1-Gbps NICs on our $k = 6$ testbed, and using 10-Gbps NICs on our three system setup. We ran a low-intensity test (roughly 50 and 300 Mbps link utilization per client and server host, respectively) and a high-intensity test (roughly 1–2 and 5–7 Gbps for client and server hosts respectively in the 10-Gbps case, and saturated links for servers in the 1-Gbps case). We noted that in all the low-intensity test cases, and in the 1-Gbps high-intensity cases, we were still able to derive a clear signal and successfully pick out the faulty link using 1-minute intervals. In our worst-case scenario of 10-Gbps links and a 16-KB send buffer size, we note a significant

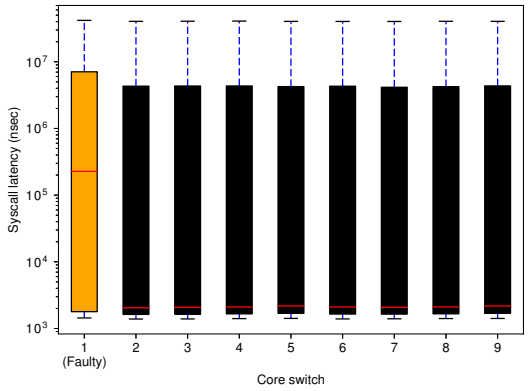

Figure 9: `select()` latency distribution per core switch for the no-offload test with CPU stress.

shifting of the distribution to the right by roughly three orders of magnitude, as predicted, as depicted in Figure 8. While the faulty-path distribution is closer to the non-faulty distributions, there is still enough divergence to clearly differentiate it from the pack, albeit requiring our statistical tests to run over longer time intervals. We note, however, that such small send socket buffer sizes are unlikely in real-world deployments.

B.4 The effect of NIC offloads

Contemporary NICs have a variety of processing offload features designed to cut down on end host CPU utilization (which we've already discussed can be heavily utilized in a datacenter environment). For example, TCP discretizes a continuous stream into individual packets determined by end to end path MTU; a feature called "TCP Segmentation Offload" allows the NIC to perform this discretization, saving the CPU the effort.

NICs typically implement three common offload features: TCP Segmentation Offload, Generic Segmentation Offload and Generic Receive Offload. All our previous experiments had these features turned on in every end host. To test the sensitivity of our approach to the availability and state of these features, we re-ran the bidirectional client-server traffic pattern with all three offload features turned off. Figure 9 depicts the `select()` latency distribution for two client hosts and one server host within our private testbed with all offloads turned off and a CPU utilization of 100% using the combination of programs described in the CPU stress test earlier. This scenario represents a sort of worst case for our approach due to the high CPU utilization required to push multiple gigabits of traffic without offload; despite this, our approach is still able to correctly flag the faulty path over a 30-second interval.

C. GENERAL-CASE TOPOLOGIES

The characteristics of the production datacenter we examined in this work lends itself to relatively simple diagnosis of which link is faulty based on per-link performance metric binning; however, alternative scenarios may exist where either traffic is not as evenly load balanced, or a different topology complicates the ability to subdivide link by hierarchy for the purposes of comparison (for example, different pods in a network might have different tree depths).

Our method fundamentally depends on finding roughly equivalent binnings for flow metrics, such that outliers can be found. In the case of a network with hotspots or complicated topologies, which can confound this process, we can still make headway by considering links at every multipath decision point as a single equivalency group. If one of these links exhibits outlier performance, the flows traversing the link can be marked individually as faulty rather than the link as a whole, and the flow and the traversed path can be submitted as input to a graph-based fault localization algorithm such as SCORE [25] or Gestalt [30]. We leave the evaluation of such a scenario to future work.